Cerebral Cortex, December 2017;27: 5557–5567

doi: 10.1093/cercor/bhw323
Advance Access Publication Date: 1 November 2016
Original Article

ORIGINAL ARTICLE

Influences of Brain Size, Sex, and Sex Chromosome Complement on the Architecture of Human Cortical Folding

Ari M. Fish[1], Arnaud Cachia[2,3], Clara Fischer[4,5], Catherine Mankiw[1], P.K. Reardon[1], Liv S. Clasen[1], Jonathan D. Blumenthal[1], Deanna Greenstein[1], Jay N. Giedd[6], Jean-François Mangin[4,5], and Armin Raznahan[1]

[1]Developmental Neurogenomics Unit, Child Psychiatry Branch, National Institute of Mental Health, Bethesda, MD 20892, USA, [2]CNRS-University Paris Descartes UMR 8240, Laboratory for the Psychology of Child Development and Education, La Sorbonne, Paris 75005, France, [3]INSERM-Paris Descartes University UMR 894, Imaging Biomarkers of Brain Development and Disorders, Ste Anne Hospital, Paris 75014, France, [4]UNATI, Neurospin, CEA, Gif-sur-Yvette 91191, France, [5]CATI Multicenter Neuroimaging Platform, Neurospin, cati-neuroimaging.com, Gif-sur-Yvette 91191, France, and [6]Department of Psychiatry, University of California, San Diego, La Jolla, CA 92093, USA

Address correspondence to Armin Raznahan, National Institute of Mental Health, NIH, 10 Center Drive, Building 10, Rm 4D18, MSC 1367, Bethesda, MD 20892, USA. Email: raznahana@mail.nih.gov

Abstract

Gyrification is a fundamental property of the human cortex that is increasingly studied by basic and clinical neuroscience. However, it remains unclear if and how the global architecture of cortical folding varies with 3 interwoven sources of anatomical variation: brain size, sex, and sex chromosome dosage (SCD). Here, for 375 individuals spanning 7 karyotype groups (XX, XY, XXX, XYY, XXY, XXYY, XXXXY), we use structural neuroimaging to measure a global sulcation index (SI, total sulcal/cortical hull area) and both determinants of sulcal area: total sulcal length and mean sulcal depth. We detail large and patterned effects of sex and SCD across all folding metrics, but show that these effects are in fact largely consistent with the normative scaling of cortical folding in health: larger human brains have disproportionately high SI due to a relative expansion of sulcal area versus hull area, which arises because disproportionate sulcal lengthening overcomes a lack of proportionate sulcal deepening. Accounting for these normative allometries reveals 1) brain size-independent sulcal lengthening in males versus females, and 2) insensitivity of overall folding architecture to SCD. Our methodology and findings provide a novel context for future studies of human cortical folding in health and disease.

Key words: allometry, gyrification, sex chromosome aneuploidy, sex differences, sulci

Cortical folding—or gyrification/sulcation—has been a longstanding focus of intense scientific study (Tiedemann 1816; His 1904) and is now recognized as a fundamental property of the human brain that can shed light on evolutionary (Zilles et al. 2013), developmental (Dubois et al. 2008; White et al. 2010; Hogstrom et al. 2012; Cachia et al. 2016) and disease-related (Cachia et al. 2008; Germanaud et al. 2014) processes. Notably, evidence from comparative anatomy suggests that the human cortex shows a

disproportionately high degree of gyrification relative to other primates after brain size is taken into account (Rogers et al. 2010; Zilles et al. 2013), and within humans, greater gyrification has been linked to increased cognitive capacity, processing speed and executive function (Hofman 2014; Gautam et al. 2015; Gregory et al. 2016).

Effective study of human brain gyrification in health and disease requires an understanding of the relationship between cortical folding and factors such as sex and overall brain size. These questions are not just important from a methodological perspective, but are also central to our basic understanding of human brain development. There is currently little consensus regarding the independent effects of sex and brain size on human brain gyrification however, and it remains unknown if brain gyrification is sensitive to sex-biased biological influences such as sex hormones or sex chromosome dosage (SCD). The potential for sex and SCD to modify cortical folding stems in part from the fact that both factors modulate brain size and cortical thickness (Giedd et al. 2012; Raznahan et al. 2014). These 2 physical properties of the brain have been identified as critical determinants of gyrification by recent biophysical (Tallinen et al. 2014) and evolutionary (Mota and Herculano-Houzel 2015) models for cortical folding.

To date, studies of sex differences in gyrification have yielded little consensus [gyrification in males > females (Raznahan et al. 2011; Gautam et al. 2015), females > males (Luders et al. 2004)], and the contribution of sex differences in brain size to these observations is also uncertain. Although there is general agreement that larger brain size is associated with greater cortical surface area and gyrification (Im et al. 2008; Toro et al. 2008; Lyall et al. 2015), it is unclear if the well-established differences in average brain size between males and females (Giedd et al. 2012) can account for any observed sex differences in cortical folding (Raznahan et al. 2011). A major obstacle to resolving this issue is the lack of integrated studies of sex and brain size effects on cortical folding that properly control for known non-linearity (allometry) in the scaling relationships between total brain volume (TBV) and cortical folding (Im et al. 2008; Toro et al. 2008; Germanaud et al. 2012). Indeed, studies of other neuroanatomical phenotypes have consistently shown that failing to quantify and account for brain allometry can drastically alter conclusions about the existence and nature of sex differences in human brain structure (Raznahan et al. 2014; Reardon et al. 2016).

Here, we use an allometric framework to characterize sex differences in cortical gyrification and the diverse set of anatomical metrics that together determine the overall extent of cortical folding. We quantify global cortical gyrification using a "Sulcation Index" (SI) (Cachia et al. 2008)—the ratio between total sulcal surface area and the surface area of the brain's outer convex hull—and then further fractionate total sulcal surface area into its 2 determinants: total sulcal length and mean sulcal depth. In addition to detailing sex differences in SI and its subcomponents, we also test whether folding metrics are sensitive to a foundational biological sex-difference with demonstrated capacity to impact cortical anatomy (Raznahan et al. 2014; Savic and Arver 2014): variation in X- and Y-chromosome dosage. We estimate SCD effects on folding metrics within a globally unique neuroimaging data set including humans with diverse sex chromosome aneuploidies (SCAs: XXX, XXY, XYY, XXYY, and XXXXY syndromes) as well as typically developing XX females and XY males. In addition to providing a powerful opportunity to model X- and Y-chromosome dosage effects on brain organization, SCAs are also important neurogenetic disorders in their own right, and show increased rates of neuropsychiatric impairment (Hong and Reiss 2014) which remain poorly understood within neurobiological terms.

To quantify the normative allometry of cortical folding as a framework for examination of sex and SCD effects, we harness a non-overlapping, independent sample of typically developing controls to directly model the scaling coefficients that interrelate variation in TBV and all folding metrics within the healthy human brain.

Materials and Methods

Participants

Our study included a total of 375 participants comprised of 1) a "core sample" of 264 individuals aged 5–25 years, representing a variety of karyotypes: 65 XX, 73 XY, 24 XXX, 52 XXY, 26 XYY, 19 XXYY, and 5 XXXXY, and 2) a non-overlapping sample of 111 typically developing individuals aged 12–14 years (48 female and 63 males), used to determine normative scaling laws for each of the folding metrics at the mean age of our core sample. Participant characteristics are detailed in Table 1.

Participants with SCA were recruited through advertisements on the NIH website and parent-support groups across the United States of America (USA). To be included in the study, participants must have had a non-mosaic, X-/Y-aneuploidy and must never have had a head injury or condition that would result in any gross brain abnormalities. Typically developing participants were all singletons recruited from the USA enrolled in a longitudinal study of typical brain development (ClinicalTrials.gov identifier: NCT00001246) (Giedd et al. 2015). To be included in the study, the normative sample participants must never have been diagnosed with a mental illness, received any mental health treatment or special education services, had a medical condition impacting the nervous system or been prescribed psychiatric medications.

Neuroimaging

All structural magnetic resonance imaging (sMRI) brain scans were T1-weighted images with contiguous 1.5mm axial slices and acquired on the same 1.5-T General Electric Signa scanner at the National Institutes of Health in Bethesda, Maryland, USA —gathered using a 3D spoiled-gradient recalled-echo sequence with the following image acquisition parameters: echo time, 5 ms; repetition time, 24 ms; flip angle, 45°; acquisition matrix, 256 × 192; number of excitations, 1; and field-of-view, 24 cm. All scans passed quality assessment by 2 independent raters for the presence of visible motion artifacts. Measures of total brain tissue volume (TBV) were derived as the sum of gray and white matter volumes generated through automated tissue classification using BrainVISA 4.5 software (Fischer et al. 2012).

Automated Sulcal Morphometry

For all scans, sulcal segmentation and identification was performed with BrainVISA 4.5 software using the Morphologist Toolbox. Briefly, this fully automated pipeline proceeds through the following steps: First, following correction of spatial signal inhomogeneities, a binary brain mask is generated using signal intensity histograms, and is then split into 3 parts corresponding to the 2 cerebral hemispheres and cerebellum. Next, a negative mold of the white matter surface is computed for each hemisphere mask, with a gray/white matter surface being derived from this mold through a topology-preserving deformation algorithm. The mold is finally skeletonized in order to

Table 1 Participant characteristics

Characteristic	Core sample							Sample for allometric analyses
	XX	XY	XXX	XXY	XYY	XXYY	XXXXY	
Sample size	65	73	24	52	26	19	5	111 (48 females/63 males)
Age [years]								
Mean (std dev)	13.1 (5.42)	13.1 (4.88)	12.1 (5.48)	13.2 (4.94)	12.6 (4.79)	14.0 (5.56)	12.9 (4.82)	13.01 (0.56)
Range	5.16–25.13	5.57–25.50	5.02–24.78	5.21–25.97	5.71–23.05	5.07–22.96	7.66–17.17	12.01–13.99
Mean IQ (std dev)								
Full scale mean*	114 (12.5)	116 (13.4)	94 (12.9)	96 (15.9)	91 (14.2)	86 (13.1)	56 (7.2)	118 (12.0)
Verbal mean*	115 (13.6)	111 (16.6)	94 (13.9)	94 (16.3)	88 (13.8)	81 (12.7)	61 (9.8)	115 (14.1)
Performance mean*	110 (11.5)	112 (13.4)	95 (13.0)	99 (15.2)	96 (16.3)	95 (12.6)	56 (2.6)	114 (12.2)
SES (std dev)								
Mean*	47 (18.8)	48 (20.9)	43 (15.6)	55 (21.3)	59 (22.3)	44 (20.3)	69 (16.8)	38 (18.8)
RACE								
Caucasian	54	64	19	48	25	17	4	94
African	4	4	0	2	0	0	0	8
Asian	1	0	1	0	0	0	0	4
Hispanic	4	2	3	1	1	1	1	3
Other	2	3	1	1	0	1	0	2
Tanner stage**								
1	17	17	7	14	8	7	2	3
2	7	11	4	9	5	3	0	12
3	9	11	5	12	7	2	1	49
4	17	13	5	8	4	6	1	34
5	13	19	3	8	2	1	0	4
Not known	2	2	0	1	0	0	1	9

Note: SES, socioeconomic status. *$P < 0.01$ for omnibus test of significant variation across groups in core sample. **$P = 0.03$ for χ^2-test for nonrandom distribution of Tanner stage between sexes in allometric sample. Within the allometric sample, females show pubertal advancement as compared with males, reflected by the distribution of Tanner stages by sex.

detect the cortical folds as crest surfaces of the 3D MR image located inside the mold. Skeletonization is a standard technique in mathematical morphology. An object is eroded until its thickness is lost; for example, a door would become a flat 2D surface or a ball with a cavity would become a sphere. The crest surfaces stem from a morphological watershed process iteratively eroding the 3D mold from the lightest intensities to the darkest intensities. Topological constraints guarantee that the resulting surfaces have no holes. The end result is a set of topologically elementary surfaces located along the darkest part of the fold corresponding to cerebrospinal fluid. These elementary surfaces are split further when a deformation of the deepest part of the fold indicates the presence of a buried gyrus. The length and the mean depth of each elementary fold were estimated. The length was calculated from the skeleton as the length of the junction between the fold and the brain hull, namely the longest geodesic distance embedded in this junction. The fold depth was the average of the shortest skeleton-based geodesic distance from the points of the bottom line of the fold to the brain hull (Mangin et al. 2004).

For each participant in our study, we summed all fold lengths to generate a total sulcal length measure, and averaged all fold depths (weighted by fold length) to derive a global measure of mean sulcal depth. Elementary fold surface areas (fold length * fold depth) were also summed to provide a measure of total sulcal surface area for each participant. The hull area is derived in native space by calculating the area of the brain mesh defined via a morphologic closing of the brain mask that ensures boundary smoothness using an isotropic closing of 10 mm, which excludes sulcal areas during definition of the exposed cortical surface area (Mangin et al. 2004). The SI for each hemisphere is the ratio between total sulcal surface area and hull area. Thus, a cortex with extensive folding has a large SI, whereas a cortex with a low degree of folding has a small SI. We averaged the left and right SI for each scan to create a bilateral measure of SI.

The above metrics allow overall cortical folding (SI) to be systematically fractionated into its 2 determinants—sulcal surface area and cortical hull area—with sulcal surface area itself being further decomposed into sulcal length and sulcal depth.

Expected Cortical Scaling Relationships

Isometric scaling relationships between measurements are based upon the null hypothesis that an object remains geometrically proportional as its size increases. These mathematical principles allow us to describe expected scaling relationships between volumetric, areal and linear measures of a 3-dimensional structure. Thus, if cortical geometry remains stable over varying brain size, areal measures (sulcal surface area and hull area) will scale to the 2/3 power of brain volume, whereas linear measures (sulcal length and depth) should scale to the 1/3 power. By extension, SI—a ratio of 2 areal metrics (surface and hull)—should remain static over varying brain size. This theoretical framework specifies null hypotheses regarding the scaling coefficient linking each folding measure to TBV (Table 2), which can be used to test for changes in cortical geometry with varying brain size.

Statistical Analyses

Participant Characteristics

Participant characteristics (Table 1) were compared across karyotype groups using ANOVA *F*-tests for continuous variables

Table 2 Allometric scaling of folding metrics in health

Measure	Expected scaling coefficient with TBV	Observed scaling coefficient with TBV	Sex offset (males vs. females)
SI	0	0.375**	
Hull area	0.666	0.706*	
Sulcal area	0.666	1.081**	
Sulcal length	0.333	0.733**	0.011*
Mean depth	0.333	0.229**	

*Indicates statistically significant difference from expected scaling ($P < 0.05$)
**Indicates statistically significant difference from expected scaling ($P < 8.9 \times 10^{-7}$).

(i.e., Full scale IQ, Verbal IQ, Performance IQ, SES) and χ^2-tests for categorical variables (i.e., Race, Tanner stage).

Sex and Sex Chromosome Effects on Raw Gyrification Metrics

We calculated the mean TBV as well as the mean value for each of the 5 folding metrics for each karyotype group in our core sample. Omnibus *F*-tests were used to assess variation in each metric across all karyotype groups. Where significant group effects were observed, post hoc *T*-tests were used to compare groups in a pairwise fashion (Fig. 1). To visualize the effect of karyotype group on folding metrics in a way that allows direct comparison across groups and metrics, we plotted observed folding metrics in each group as effect size shifts relative to a common reference group—XY males (Fig. 2).

For each folding metric, we used linear models in selected karyotype group subsets to directly test for interactions between X-chromosome dosage and 1) gonadal sex (subset: XY, XXY, XX, XXX), 2) and Y-chromosome aneuploidy (subset: XY, XXY, XYY, XXYY). These models were specified as follows (using the test for interaction between X-dosage and SEX as an example):

$$\text{Folding Metric} = \beta 0 + \beta 1(\text{Xdose}) + \beta 2(\text{SEX}) + \beta 3(\text{Xdose} \times \text{SEX}),$$

where Xdose and SEX are binary variables encoding 1) the presence versus absence of a supernumerary X-chromosome, and 2) gonadal sex (male vs. female), respectively. Failure to reject the null hypothesis that $\beta 3 = 0$ was interpreted as Xdose effects being equivalent in both sexes.

Normative Allometry of Cortical Folding

Using a well-established log–log approach (Gould 1966; Reardon et al. 2016), we calculated allometric scaling norms for all folding metrics within a separate sample of 111 typically developing XY males and XX females. To systematically consider all potential contributions of sex to variation in folding, we used the following step-wise approach. We first tested for significant sex differences in the scaling of each folding metric with TBV using the following model:

$$\log 10(\text{Folding Metric}) = \beta 0 + \beta 1[\log 10(\text{TBV})] + \beta 2(\text{SEX}) + \beta 3[\log 10(\text{TBV}) \times \text{SEX}] \quad (1)$$

With no observed sex differences in the scaling (i.e., failure to reject null hypothesis that $\beta 3 = 0$), we asked if there were any baseline sex differences in each folding metric across TBVs:

$$\log 10(\text{Folding Metric}) = \beta 0 + \beta 1[\log 10(\text{TBV})] + \beta 2(\text{SEX}) \quad (2)$$

Finally, in the absence of any such sex offset (i.e., failure to reject null that $\beta 2 = 0$), variation in each folding metric was related to TBV alone:

$$\log 10(\text{Folding metric}) \sim \beta 0 + \beta 1 \times \log 10(\text{TBV}). \quad (3)$$

For each folding metric, observed $\beta 1$ values for the appropriate model were compared against the null value that would be expected if geometric proportions of cortical scaling remained constant over brain size (see above, and Table 2). $\beta 1$ values below and above the null were considered to indicate hypo- and hyperallometry, respectively, with values that were statistically indistinguishable from the null indicating isometric scaling.

Sex and Sex Chromosome Effects in the Context of Allometry

After producing scaling norms for each folding metric within our normative sample, we assessed whether the observed mean value of each folding metric per SCA group deviated from, or conformed to, what would be predicted from the mean TBV of that group given normative scaling. Relationships between observed and predicted values were visualized by plotting the mean (±95% confidence interval) of each folding metric for all karyotype groups atop the normative scaling data. Differences between observed and predicted values were assessed using *T*-tests, with associated *P*-values corrected for multiple comparisons (5 separate comparisons for each measure) using the Bonferroni method.

We also carried out a separate set of analyses that directly tested whether scaling relationships between folding metrics and TBV vary across karyotype groups within our core sample. This was achieved by first modeling TBV and all folding metrics in our core sample using the following equation:

$$\text{Folding Metric} = \beta 0 + \beta 1(\text{GROUP}) + \beta 2(\text{AGE}) + \beta 3(\text{GROUP} \times \text{AGE}).$$

Then, for each individual within our core sample, we calculated the difference between his/her expected and observed values of TBV, SI, hull area, sulcal area, sulcal length, and sulcal depth. Next, after adding back group mean values for each metric depending on the individual's karyotype, we used a log–log framework to test if observed scaling relationships between TBV and folding metrics vary across karyotype groups in our core sample. Specifically, each residualized folding metric was modeled using the following equation:

$$\log 10(\text{residualized Folding Metric}) = \beta 0 + \beta 1\,(\text{GROUP}) + \beta 2\,[\log 10(\text{residualized TBV})] + \beta 3\,[\text{GROUP} \times \log 10(\text{residualized TBV})]$$

An *F*-test for the $\beta 3$ term in this model was used to determine if karyotype group modifies scaling relationships between TBV and each folding metric.

Results

Sex and Sex Chromosome Effects on Raw Gyrification Metrics

As a starting point, and to facilitate comparison with other work, we charted the effects of sex and SCD on absolute TBV, SI and the determinants of SI—sulcal surface area, hull area, sulcal length, and sulcal depth. All metrics differed significantly across karyotype groups (Fig. 1).

CHARACTERISTIC	KARYOTYPE							Omnibus test for group differences	
	XX	XY	XXX	XXY	XYY	XXYY	XXXXY	F-statistic	p-value
TBV (cm^3)									
Mean	1262.86	1377.41	1161.96	1272.92	1391.73	1277.91	1081.49	18.36	$<2.20 \times 10^{-16}$
S.E.M	11.51	13.87	22.56	18.93	25.31	26.97	26.12		
Sulcation Index									
Mean	2.21	2.28	2.18	2.19	2.31	2.19	2.19	3.74	1.377×10^{-3}
S.E.M	0.02	0.02	0.04	0.02	0.03	0.03	0.05		
Hull Area (cm^2)									
Mean	806.78	860.76	778.59	830.25	878.92	843.72	776.72	12.85	1.08×10^{-12}
S.E.M	5.13	6.60	10.92	9.76	11.59	13.58	23.04		
Sulcal Area (cm^2)									
Mean	1788.95	1962.04	1705.52	1820.20	2033.94	1846.01	1606.68	11.39	2.73×10^{-11}
S.E.M	25.15	23.30	46.78	29.36	40.95	41.52	60.63		
Total Length (cm)									
Mean	716.32	772.88	693.75	733.19	799.31	739.82	681.44	11.40	2.705×10^{-11}
S.E.M	7.77	7.20	14.31	8.98	12.32	14.99	24.44		
Mean Depth (cm)									
Mean	1.184	1.205	1.179	1.188	1.204	1.200	1.145	4.87	9.794×10^{-5}
S.E.M	0.004	0.004	0.008	0.005	0.007	0.005	0.014		

Post-hoc pairwise T-test

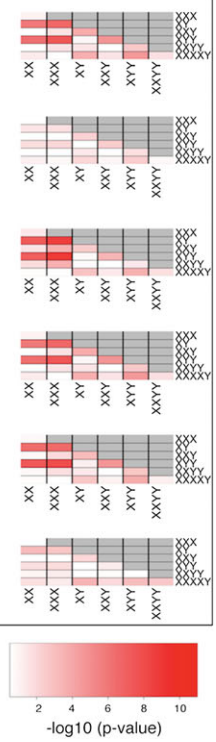

Figure 1. TBV and folding metrics across sex chromosome karyotype groups. Means and standard errors for TBVs and folding metrics within each core sample karyotype group, alongside post hoc pairwise heatmaps for each karyotype comparison. The color bar indicates the level of significance for each karyotype pair.

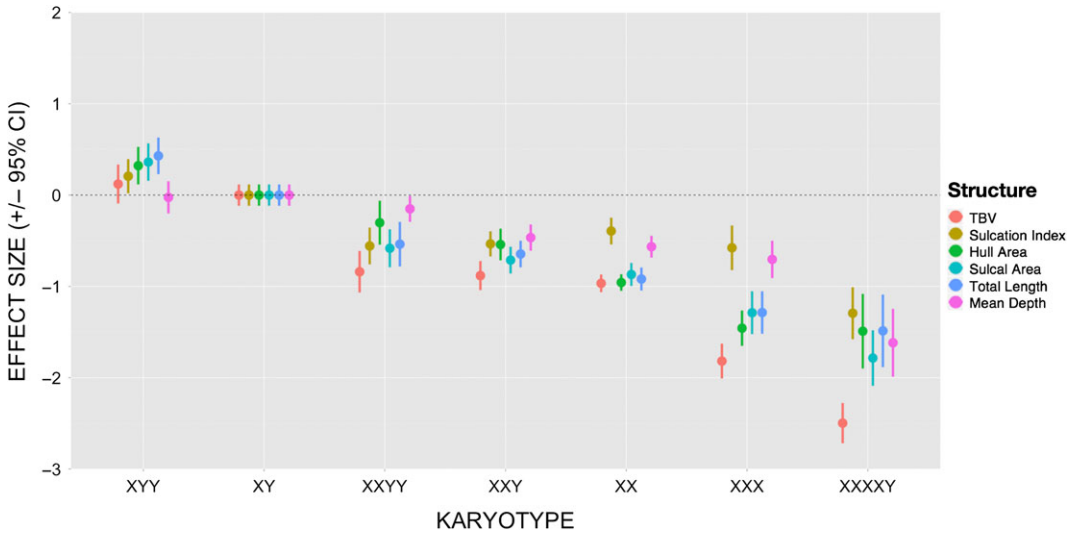

Figure 2. Effect size shifts for TBV and folding metrics across sex chromosome karyotype groups. Standardized effect size graph of TBV, SI, hull area, surface area, total length, and total mean depth for each karyotype group, expressed as the mean (±95% confidence interval) effect size deviation relative to distributions in XY males.

With respect to normative sex differences, we found that TBV, SI and all SI determinants were significantly reduced in typically developing females relative to typically developing males (Figs 1 and 2). Reductions of hull area, surface area and sulcal length in XX females versus XY males were all of comparable effect size to observed reductions in TBV (~1 standard deviation shift), while smaller effect size reductions were seen for SI and sulcal depth in XX females relative to XY males.

With regard to SCD effects, visualization of brain size and cortical folding changes in SCA groups (Fig. 2) and post hoc pairwise group comparisons for each metric (Fig. 1) revealed 1) dissociable SCD effects across different anatomical measures, and 2) a general divergence between X- and Y-chromosome dosage effects on cortical folding. First, supernumerary X-chromosomes were associated with reductions in TBV and all folding metrics (e.g., in the contrast between XXY and XY males, and between

XXX and XX females), but these reductions were greater in magnitude and more consistent across groups for TBV, hull area, sulcal area, and sulcal length than for SI and sulcal depth. TBV, hull area, sulcal area, and sulcal length also showed more evidence of a step-wise decrease with increasing X-chromosome dose than was apparent for SI and sulcal depth. Second, visualization of effect sizes across karyotype groups indicated that the presence of a supernumerary Y-chromosome had an opposite effect on most folding metrics than the presence of a supernumerary X-chromosome (increase and decrease, respectively). This divergence in X- and Y-chromosome effects on folding metrics is well illustrated by the comparison between observed anatomical changes in XYY and XXY groups relative to XY males (Figs 1 and 2).

Supplementary sensitivity analyses established that for all anatomical metrics examined, X-dosage effects were not significantly modified by 1) gonadal sex [tested using 2-factor (sex and X-aneuploidy) ANOVA across XX, XXX, XY, and XXY groups], or 2) Y-chromosome dosage [tested using 2-factor (X-aneuploidy and Y-aneuploidy) ANOVA across XY, XXY, XYY, and XXYY groups].

Normative Allometry of Cortical Folding

Scaling relationships between folding metrics and brain size variation in health were quantified in our non-overlapping sample of typically developing males and females. We found that SI and its determinants differed markedly from each other in the degree to which they adhered to the scaling relationships that would be predicted under the null hypothesis of stable cortical folding geometry with varying brain size (Table 2, Fig. 3). Specifically, we found that SI increased with increasing TBV. This hyperallometric scaling of SI with TBV was driven by a clearly disproportionate expansion of sulcal area with increasing TBV (predicted vs. observed scaling coefficient: 0.66 vs. 1.08) coupled with a near proportionate expansion of hull area (predicted vs. observed scaling coefficient: 0.66 vs. 0.71).

Allometric analysis of the 2 lower-order metrics that determine sulcal area—sulcal length and depth—revealed that disproportionate expansion of sulcal area with increasing TBV arises through a hyperallometric scaling relationship between sulcal length and TBV, which compensates for a hypo-allometric scaling of sulcal depth with TBV.

Sex and Sex Chromosome Effects in the Context of Allometry

Our allometric analyses indicated that the scaling relationships observed for SI and its determinants are not sexually dimorphic, but did reveal a significant "sex-offset" effect for sulcal length. Estimated sulcal length was greater in males than females across all TBV values represented in our study (Table 2). This significant sex-offset for sulcal length was associated with a commensurate, but statistically non-significant, trend towards greater sulcal area and SI in males versus females for a given TBV ($P = 0.06$ and $P = 0.132$, respectively).

Having charted the complex relationship between brain size and different elements of cortical folding in health, we asked if the highly patterned impact of X- and Y-chromosome dosage on SI and its determinants fell within allometric expectations, or represented a disruption of normal folding geometry. These analyses indicated that the observed changes in SI and SI determinants across all SCA groups are commensurate with observed TBV changes. This conclusion was supported for each folding metric by both visualization of observed versus expected values in each karyotype group (Fig. 4), and statistical comparison of observed versus expected values using t-tests (P-values for all comparisons > 0.05 after Bonferroni correction for multiple comparisons across 5 karyotype groups). Separate analyses within our core sample further demonstrated that scaling relationships between TBV and folding metrics (after appropriate residualization of all metrics for age and group effects) do not show statistically significant variation as a function of karyotype group (Table 3).

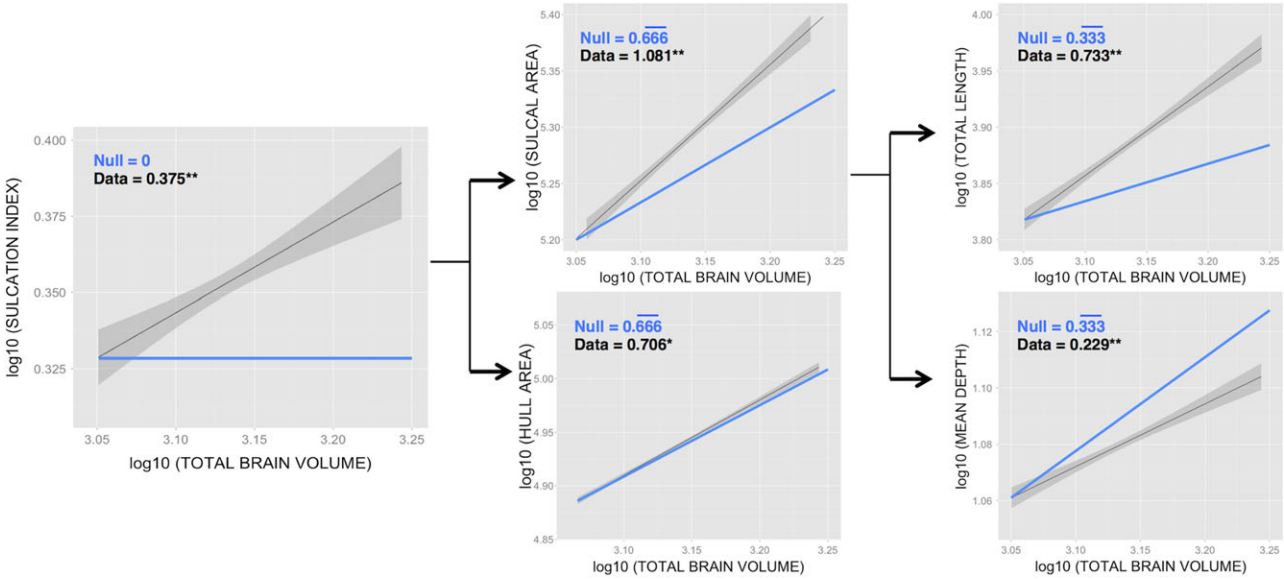

Figure 3. Log–log allometric scaling of observed versus expected scaling for folding metrics relative to TBV within the normative sample. * indicates statistically significant difference from expected scaling ($P < 0.05$). ** indicates statistically significant difference from expected scaling ($P < 8.9 \times 10^{-7}$). Log–log allometric scaling graphs of observed (black) versus expected (blue) scaling relationships for each folding metric with respect to TBV. "Null" values represent the expected scaling coefficient given geometric scaling norms, whereas the "data" value represents the observed scaling coefficient.

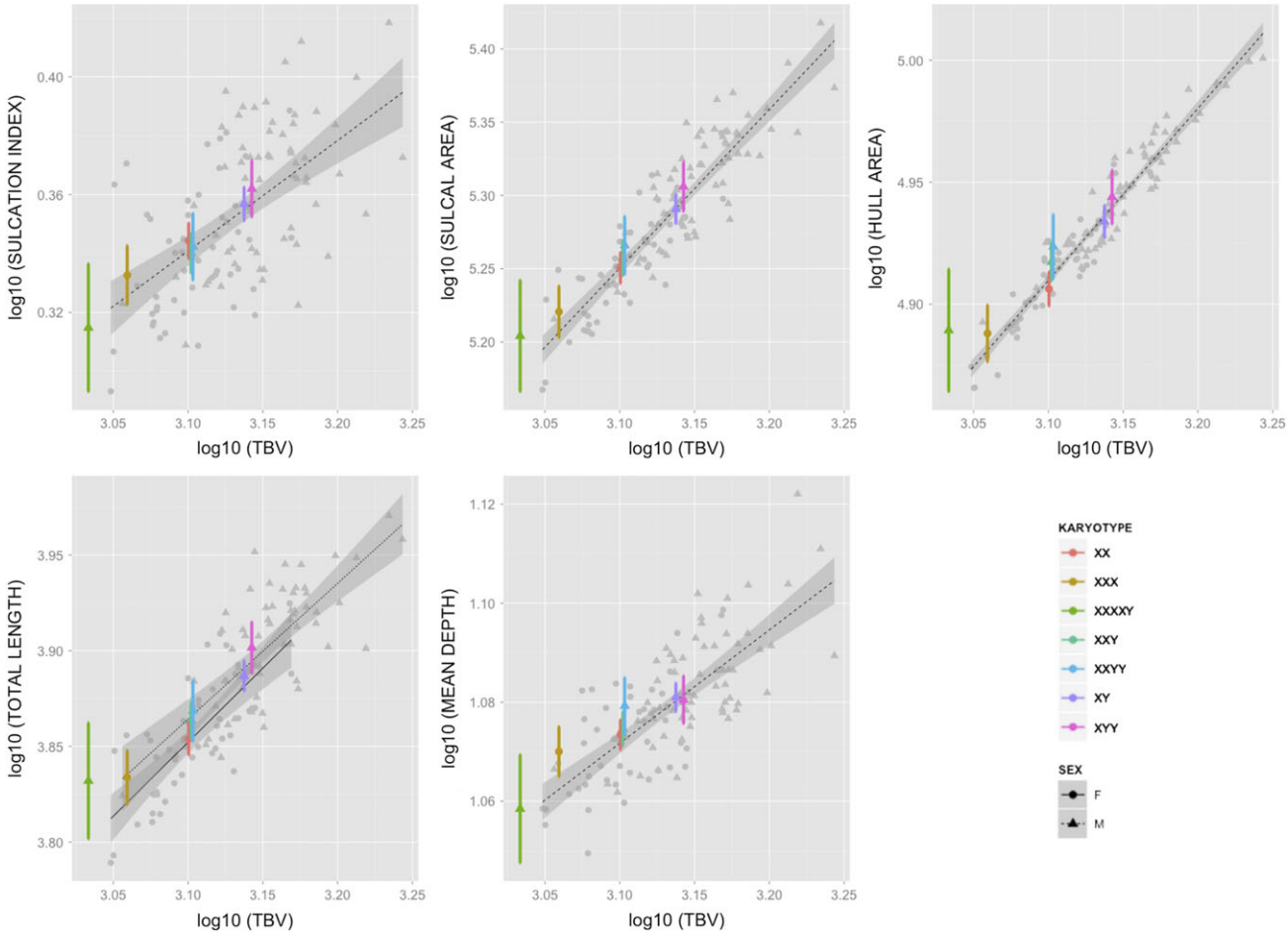

Figure 4. Log–log allometric scaling of normative sample with karyotype group means. Means of each folding metric for the SCA groups atop the log–log allometric scaling of the normative sample. Background gray points represent typically developing males (triangles) and females (circles) in the non-overlapping sample used to define scaling norms linking each folding metric to TBV (black fit lines). Superimposed colored points and ranges denote observed mean folding metrics (±95% confidence intervals) at the mean TBV of each karyotype group.

Table 3 Allometric scaling relationships between residualized TBV and folding metrics in core sample

Measure	Test for karyotype group differences in scaling with TBV in "core" sample
SI	$F_{6,250} = 0.5$, $P = 0.8$
Hull area	$F_{6,250} = 1.2$, $P = 0.3$
Sulcal area	$F_{6,250} = 0.3$, $P = 0.9$
Sulcal length	$F_{6,250} = 0.3$, $P = 0.9$
Mean depth	$F_{6,250} = 0.1$, $P = 0.99$

Note the lack of statistically significant variation in allometry across karyotype groups for SI or any of its determinants.

Discussion

Sex and Sex Chromosome Effects on Raw Gyrification Metrics

Our comparison of typically developing males and females replicates known sex differences (male > female) in TBV, cortical surface area and raw global gyrification (Raznahan et al. 2011; Giedd et al. 2012), and further fractionates gyrification to establish that males achieve greater raw SI through increases in both mean sulcal depth and total sulcal length. We are not aware of any published studies examining sex differences in absolute sulcal length, and both existent studies examining sex differences in absolute sulcal depth have considered individual sulci in adulthood and failed to find statistically significant male–female differences (Kochunov et al. 2005; Cykowski et al. 2008). Although we find that the absolute value of all measured folding metrics is greater in males than females, the effect size of statistically significant sex differences varies across different aspects of gyrification, with global SI and sulcal depth showing weaker sex differences than TBV, sulcal area, and sulcal length.

Analysis of SCD reveals divergent X- and Y-chromosome effects on raw folding metrics (decreasing and increasing metrics, respectively) in keeping with the opposing effects of X- and Y-chromosome dosage on overall brain size and total cortical surface area (Raznahan et al. 2014). Echoing our finding for sex-effects, SCA effects are not homogenous in their magnitude across all folding metrics, with overall SI and sulcal depth tending to show relatively smaller effect size shifts with SCD changes than sulcal area or length. The diversity of SCAs represented in our study allows us to establish that X-chromosome effects on raw folding metrics show a step-wise, "dose-response" relationship, and are not significantly modified by gonadal sex or Y-chromosome dosage, strengthening the case that these effects index a primary influence of chromosome dosage (e.g., vs.

secondary endocrine changes). However, since the only prior study of global gyrification in SCA reported that X-monosomy reduces cortical folding in females (Raznahan et al. 2010), X-chromosome dosage effects on folding may be non-linear in the transition between haploinsufficiancy and supernumeracy.

While the above findings help to clarify sex and SCD effects on raw folding metrics, interpretation of these effects is fundamentally altered by our allometric analyses, which identify profoundly non-linear and heterogeneous relationships between brain folding metrics and brain size.

Normative Allometry of Cortical Folding

We find a strong positive relationship between global SI and increasing brain size in humans, which contrasts with the only prior study of this global metric. This prior study used a smaller sample of postmortem brains and concluded that global cortical folding is insensitive to brain size (Zilles et al. 1988). Changes in SI with brain size can only be achieved if sulcal surface area and cortical hull area are differentially related to TBV. Our data clarify that the gross hyperallometry of total sulcal area (also see Im et al. 2008; Toro et al. 2008) is accompanied by a near isometric scaling relationship between the cortical convex hull and TBV, which together fully explain the observed increases in SI with TBV. The mechanisms underlying the hyperallometric scaling of cortical surface area in humans remain unknown. Hyperallometry of cortical surface area with TBV across species (Prothero and Sundsten 1984) has been argued to arise from expansion of progenitor cell pool size in early cortical development (Rakic 1988; Lui et al. 2011; Fernández et al. 2016), although it is unclear whether similar or distinct mechanisms contribute to the hyperallometry of sulcal surface area with intraspecific TBV increases in humans.

By fractionating total sulcal surface area into its 2 determinants of sulcal length and sulcal depth, we are able to further specify the geometric source of disproportionate overall cortical folding in larger brains to a disproportionate increase in total sulcal length. The degree of this sulcal length hyperallometry is great enough to counteract the failure of sulcal depth to increase in proportion with TBV. We speculate that the hyperallometry of sulcal length predominantly reflects increased sulcal tortuosity in larger brains, given that 1) spectral analysis of the cortical surface in humans has established that frequencies representative of the intra-sulcal "twisting" and "dimpling" of sulci show strongly hyperallometric relationships with TBV that are not seen for frequencies representative of sulcal folds themselves (Germanaud et al. 2012), and 2) absolute mean curvature of sulcal walls has been shown to scale hyperallometrically with TBV in adults (Im et al. 2008). Disproportionate increase in sulcal length with larger TBV could also conceivably arise through addition of more folds, although testing this hypothesis would first require major advances in our understanding of population-level variability in human sulcal typologies across development (Ono et al. 1990).

Sex and Sex Chromosome Effects in the Context of Allometry

Re-examination of normative sex differences in folding within an allometric framework clarifies that the strong and patterned effects of sex on raw SI and SI determinants are mostly commensurate with males having greater TBV than females. Thus—in recapitulation of earlier findings by Dubois et al. (2008) when examining global folding metrics in preterm newborns—sex differences in overall SI are in keeping with sex differences in overall brain size, and are not reflective of a superadded effect of sex, per se. However, we detect significant sex differences in total sulcal length (males > females) that cannot be accounted for by sex differences in TBV. The 3 dominant theoretical models for the establishment of cortical folds (reviewed in Ronan and Fletcher 2015) each offer distinct testable hypotheses regarding the mechanisms that underlie sex differences in sulcal length, including male–female differences in 1) cortico-cortical connectivity ("Axonal Tension Hypothesis"; Van Essen 1997), 2) differential expansion of supragranular versus infragranular cortical layers in development ("Radial Expansion Hypothesis"; Richman et al. 1975), and 3) cytoarchitectonic patterning of the cortical sheet ("Differential Tangential Expansion Hypothesis"; Ronan et al. 2014). Also, the recent observation that global cortical folding within the animal kingdom scales in proportion to cortical thickness and surface area (Mota and Herculano-Houzel 2015) raises a fourth testable hypothesis: sex differences in sulcal tortuosity may arise through males having thinner cortices than females during the early developmental phase of explosive cortical surface area expansion (Rajagopalan et al. 2011; Li et al. 2013). Indeed, sex differences in the relative timing of cortical area and thickness maturation have already been described during late childhood and adolescence (Raznahan et al. 2011). The hypothesis that known sex differences in cortical thickness and brain size might underlie the sex differences in sulcal length which we identify in the current study is also consistent with a recently published biophysical model for cortical folding (Tallinen et al. 2014). Under this model, sex differences in the coordination of mean cortical thickness change with tangential areal expansion of the cortical sheet during development—such as those that have been reported in infancy (Lyall et al. 2015) and late childhood (Raznahan et al. 2011)—would be predicted to impact sex differences in global gyrification. The seminal "Radial Unit Hypothesis" (Rakic 1988; Bystron et al. 2008) represents a fundamental theoretical framework for tests of the above hypotheses, as it details specific cellular processes thought to underpin cortical surface area expansion in development.

Our analyses in SCA indicate that changes in X- and Y-chromosome dosage impact cortical folding in a manner that is entirely commensurate with the divergent shifts that they induce in TBV (decrease vs. increase, respectively). Thus, normative sex differences in SCD could account for sex differences in raw folding metrics through their effect on overall brain size, but are less likely to account for the TBV-independent male–female difference in sulcal length. The fact that SCD changes do not exert a targeted effect on cortical folding echoes our prior results regarding the preservation of global cortical thickness asymmetry patterns in SCA (Lin et al. 2015). Thus, it appears that despite the ability of changes in SCD to dramatically modify overall brain size and specific structural properties of the cortex (local thickness and surface area; Raznahan et al. 2014) and subcortex (striato-thalamic shape; Reardon et al. 2016), specific aspects of early brain patterning such as the cortical sulcation and asymmetry (Habas et al. 2012) remain resilient to gross changes in X- and Y-chromosome dosage.

It is important to highlight the capacity of allometric analysis to reframe the patterned effects of SCD on raw folding metrics as being a predictable consequence of the shifts in overall brain size that accompany changes in X- and Y-chromosome dosage. A complementary mechanistic account for this preservation of global folding in SCA is offered by

biophysical theories of cortical folding (Tallinen et al. 2014), which mathematically link varied gyrification across Mammalia to the combined non-linear influences of varying brain size (with greater brain size indexing greater tangential expansion of the cortical mantle and underlying white matter) and cortical thickness (with disproportionately thick/thin cortex for a given brain size leading to disproportionately decreased/increased folding). This biophysical framework provides an overarching explanation that integrates 1) our past finding that SCA shifts brain size while preserving the inter-relationship between brain size and overall mean cortical thickness (Raznahan et al. 2014), and 2) our current finding that SCA does not distort the global architecture of cortical folding.

Limitations and Future Directions

Our findings should be considered in light of study limitations. First, our cross-sectional design is not able to resolve whether the effects of sex, brain size, and SCD on cortical folding change with age; these questions will be important targets for future longitudinal research. Longitudinal analysis of SCD effects is challenged by the relative rarity of SCA groups, but will become feasible as clinical cohorts grow in size. Although the analytic approach and associated inferences in our study do not rely on the assumption that sex and SCA influence brain anatomy in a developmentally static manner, they point towards the need for gathering the large-scale developmental data sets required to address the outstanding question of whether sex and SCA modify the "inter-relationship" between brain size and folding in a developmentally static or dynamic manner. Secondly, some previously studied scalar (e.g., mean overall cortical thickness) and composite [e.g., $(\text{cortical thickness})^{1/2} \times (\text{total cortical surface area})$] predictors of global gyrification were not examined in our study. This reflects the fact that 1) these variables have typically been examined in studies that span inter-species variation in folding (Tallinen et al. 2014; Mota and Herculano-Houzel 2015) rather than the intraspecific differences in folding that are the focus of our study, and 2) the global folding metrics examined in our study provide a concrete, self-contained and fully nested set of scalar brain measures that together fractionate overall gyrification into its mutually informative subcomponents. Finally, our study focuses on global folding rather than examining folding at the sulcal (Mangin et al. 2004) or "vertex" (Im et al. 2008) level. However, we believe that the global analyses presented here provide an integrated view of cortical organization, and a necessary foundation—theoretically, empirically and methodologically—for the analysis of more local features of folding. Perhaps the most fundamental challenge for analysis of local folding is the current lack of a comprehensive survey of the diversity of cortical folding typologies in humans. Folding typologies are established during prenatal life, appear to persist postnatally (Cachia et al. 2016), and show strong associations with other neuroanatomical (Fornito et al. 2004), cognitive (Cachia et al. 2013; Borst et al. 2016), and clinical (Nakamura et al. 2007; Plaze et al. 2015) phenotypes. Future characterization of sulcal typologies in health and SCA would set the stage for valid analyses of quantitative folding metrics at the local level.

Despite the above limitations, our study maps the normative allometry of diverse cortical folding metrics and highlights changes in sulcal length as a key driver of cortical surface area and sulcation hyperallometry in health. These normative data critically reframe the striking effects of sex and SCD on all raw cortical folding metrics, and 1) reveal a relative sulcal lengthening in typically developing males versus females that is not in keeping with male–female differences in TBV, and 2) show that global cortical folding appears to be robust to changes in X- and Y-chromosome dose across multiple SCAs.

Funding

This work was supported by the Intramural Research Program of the NIMH (ZIAMH002794-13).

Notes

The authors thank the participants and families who took part in this study. *Conflict of Interest*: None declared.

References

Borst G, Cachia A, Tissier C, Ahr E, Simon G, Houdé O. 2016. Early cerebral constraints on reading skills in school-age children: an MRI study. Mind Brain Educ. 10:47–54.

Bystron I, Blakemore C, Rakic P. 2008. Development of the human cerebral cortex: Boulder Committee revisited. Nat Rev Neurosci. 9:110–122.

Cachia A, Borst G, Tissier C, Fisher C, Plaze M, Gay O, Rivière D, Gogtay N, Giedd J, Mangin J-F, et al. 2016. Longitudinal stability of the folding pattern of the anterior cingulate cortex during development. Dev Cogn Neurosci. 19: 122–127.

Cachia A, Borst G, Vidal J, Fischer C, Pineau A, Mangin J-F, Houdé O. 2013. The shape of the ACC contributes to cognitive control efficiency in preschoolers. J Cogn Neurosci. 26: 96–106.

Cachia A, Paillère-Martinot M-L, Galinowski A, Januel D, de Beaurepaire R, Bellivier F, Artiges E, Andoh J, Bartrés-Faz D, Duchesnay E, et al. 2008. Cortical folding abnormalities in schizophrenia patients with resistant auditory hallucinations. NeuroImage. 39:927–935.

Cykowski MD, Coulon O, Kochunov PV, Amunts K, Lancaster JL, Laird AR, Glahn DC, Fox PT. 2008. The central sulcus: an observer-independent characterization of sulcal landmarks and depth asymmetry. Cereb Cortex. 18:1999–2009.

Dubois J, Benders M, Cachia A, Lazeyras F, Leuchter RH-V, Sizonenko SV, Borradori-Tolsa C, Mangin JF, Hüppi PS. 2008. Mapping the early cortical folding process in the preterm newborn brain. Cereb Cortex. 18:1444–1454.

Fernández V, Llinares-Benadero C, Borrell V. 2016. Cerebral cortex expansion and folding: what have we learned? EMBO J. 35:1021–1044.

Fischer C, Operto G, Laguitton S, Perrot M, Denghien I, Rivière D, Mangin J-F. 2012. Morphologist 2012: the new morphological pipeline of BrainVISA. Presented at the Human Brain Mapping Conference.

Fornito A, Yücel M, Wood S, Stuart GW, Buchanan J-A, Proffitt T, Anderson V, Velakoulis D, Pantelis C. 2004. Individual differences in anterior cingulate/paracingulate morphology are related to executive functions in healthy males. Cereb Cortex. 14:424–431.

Gautam P, Anstey KJ, Wen W, Sachdev PS, Cherbuin N. 2015. Cortical gyrification and its relationships with cortical volume, cortical thickness, and cognitive performance in healthy mid-life adults. Behav Brain Res. 287: 331–339.

Germanaud D, Lefèvre J, Fischer C, Bintner M, Curie A, des Portes V, Eliez S, Elmaleh-Bergès M, Lamblin D, Passemard

S, et al. 2014. Simplified gyral pattern in severe developmental microcephalies? New insights from allometric modeling for spatial and spectral analysis of gyrification. NeuroImage. 102 (Pt 2):317–331.

Germanaud D, Lefèvre J, Toro R, Fischer C, Dubois J, Hertz-Pannier L, Mangin J-F. 2012. Larger is twistier: spectral analysis of gyrification (SPANGY) applied to adult brain size polymorphism. NeuroImage. 63:1257–1272.

Giedd JN, Raznahan A, Alexander-Bloch A, Schmitt E, Gogtay N, Rapoport JL. 2015. Child psychiatry branch of the national institute of mental health longitudinal structural magnetic resonance imaging study of human brain development. Neuropsychopharmacology. 40:43–49.

Giedd JN, Raznahan A, Mills KL, Lenroot RK. 2012. Review: magnetic resonance imaging of male/female differences in human adolescent brain anatomy. Biol Sex Differ. 3: 19.

Gould SJ. 1966. Allometry and size in ontogeny and phylogeny. Biol Rev. 41:587–638.

Gregory MD, Kippenhan JS, Dickinson D, Carrasco J, Mattay VS, Weinberger DR, Berman KF. 2016. Regional variations in brain gyrification are associated with general cognitive ability in humans. Curr Biol. 26:1301–1305.

Habas PA, Scott JA, Roosta A, Rajagopalan V, Kim K, Rousseau F, Barkovich AJ, Glenn OA, Studholme C. 2012. Early folding patterns and asymmetries of the normal human brain detected from in utero MRI. Cereb Cortex. 22:13–25.

His W. 1904. Die Entwicklung des menschlichen Gehirns wahrend der ersten Monate. Leipzig: Hirzel.

Hofman MA. 2014. Evolution of the human brain: when bigger is better. Front Neuroanat. 8:15.

Hogstrom LJ, Westlye LT, Walhovd KB, Fjell AM. 2012. The structure of the cerebral cortex across adult life: age-related patterns of surface area, thickness, and gyrification. Cereb Cortex. 23:2521–2530.

Hong DS, Reiss AL. 2014. Cognitive and neurological aspects of sex chromosome aneuploidies. Lancet Neurol. 13: 306–318.

Im K, Lee J-M, Lyttelton O, Kim SH, Evans AC, Kim SI. 2008. Brain size and cortical structure in the adult human brain. Cereb Cortex. 18:2181–2191.

Kochunov P, Mangin J-F, Coyle T, Lancaster J, Thompson P, Rivière D, Cointepas Y, Régis J, Schlosser A, Royall DR, et al. 2005. Age-related morphology trends of cortical sulci. Hum Brain Mapp. 26:210–220.

Li G, Nie J, Wang L, Shi F, Lin W, Gilmore JH, Shen D. 2013. Mapping region-specific longitudinal cortical surface expansion from birth to 2 years of age. Cereb Cortex. 23: 2724–2733.

Lin A, Clasen L, Lee NR, Wallace GL, Lalonde F, Blumenthal J, Giedd JN, Raznahan A. 2015. Mapping the stability of human brain asymmetry across five sex-chromosome aneuploidies. J Neurosci. 35:140–145.

Luders E, Narr KL, Thompson PM, Rex DE, Jancke L, Steinmetz H, Toga AW. 2004. Gender differences in cortical complexity. Nat Neurosci. 7:799–800.

Lui JH, Hansen DV, Kriegstein AR. 2011. Development and evolution of the human neocortex. Cell. 146:18–36.

Lyall AE, Shi F, Geng X, Woolson S, Li G, Wang L, Hamer RM, Shen D, Gilmore JH. 2015. Dynamic development of regional cortical thickness and surface area in early childhood. Cereb Cortex. 25:2204–2212.

Mangin JF, Riviere D, Cachia A, Duchesnay E, Cointepas Y, Papadopoulos-Orfanos D, Collins DL, Evans AC, Regis J. 2004. Object-based morphometry of the cerebral cortex. IEEE Trans Med Imaging. 23:968–982.

Mota B, Herculano-Houzel S. 2015. Cortical folding scales universally with surface area and thickness, not number of neurons. Science. 349:74–77.

Nakamura M, Nestor PG, McCarley RW, Levitt JJ, Hsu L, Kawashima T, Niznikiewicz M, Shenton ME. 2007. Altered orbitofrontal sulcogyral pattern in schizophrenia. Brain. 130: 693–707.

Ono M, Kubik S, Abernathey CD. 1990. Atlas of the cerebral sulci. New York: Thieme Medical Publishers.

Plaze M, Mangin J-F, Paillère-Martinot M-L, Artiges E, Olié J-P, Krebs M-O, Gaillard R, Martinot J-L, Cachia A. 2015. "Who is talking to me?"—Self-other attribution of auditory hallucinations and sulcation of the right temporoparietal junction. Schizophr Res. 169:95–100.

Prothero JW, Sundsten JW. 1984. Folding of the cerebral cortex in mammals. A scaling model. Brain Behav Evol. 24: 152–167.

Rajagopalan V, Scott J, Habas PA, Kim K, Corbett-Detig J, Rousseau F, Barkovich AJ, Glenn OA, Studholme C. 2011. Local tissue growth patterns underlying normal fetal human brain gyrification quantified in utero. J Neurosci. 31: 2878–2887.

Rakic P. 1988. Specification of cerebral cortical areas. Science. 241:170–176.

Raznahan A, Cutter W, Lalonde F, Robertson D, Daly E, Conway GS, Skuse DH, Ross J, Lerch JP, Giedd JN, et al. 2010. Cortical anatomy in human X monosomy. Neuroimage. 49:2915–2923.

Raznahan A, Lee NR, Greenstein D, Wallace GL, Blumenthal JD, Clasen LS, Giedd JN. 2014. Globally divergent but locally convergent X- and Y-chromosome influences on cortical development. Cereb Cortex. 26:70–79.

Raznahan A, Shaw P, Lalonde F, Stockman M, Wallace GL, Greenstein D, Clasen L, Gogtay N, Giedd JN. 2011. How does your cortex grow? J Neurosci. 31:7174–7177.

Reardon PK, Clasen L, Giedd JN, Blumenthal J, Lerch JP, Chakravarty MM, Raznahan A. 2016. An allometric analysis of sex and sex chromosome dosage effects on subcortical anatomy in humans. J Neurosci. 36:2438–2448.

Richman DP, Stewart RM, Hutchinson JW, Caviness VS. 1975. Mechanical model of brain convolutional development. Science. 189:18–21.

Rogers J, Kochunov P, Zilles K, Shelledy W, Lancaster J, Thompson P, Duggirala R, Blangero J, Fox PT, Glahn DC. 2010. On the genetic architecture of cortical folding and brain volume in primates. NeuroImage. 53:1103–1108.

Ronan L, Fletcher PC. 2015. From genes to folds: a review of cortical gyrification theory. Brain Struct Funct. 220: 2475–2483.

Ronan L, Voets N, Rua C, Alexander-Bloch A, Hough M, Mackay C, Crow TJ, James A, Giedd JN, Fletcher PC. 2014. Differential tangential expansion as a mechanism for cortical gyrification. Cereb Cortex. 24:2219–2228.

Savic I, Arver S. 2014. Sex differences in cortical thickness and their possible genetic and sex hormonal underpinnings. Cereb Cortex. 24:3246–3257.

Tallinen T, Chung JY, Biggins JS, Mahadevan L. 2014. Gyrification from constrained cortical expansion. Proc Natl Acad Sci. 111:12667–12672.

Tiedemann F. 1816. Anatomie und Bildungsgeschichte des Gehirns im Foetus des Menschen: nebst einer vergleichenden Darstellung des Hirnbaues in den Thieren. Nürnberg: Stein.

Toro R, Perron M, Pike B, Richer L, Veillette S, Pausova Z, Paus T. 2008. Brain size and folding of the human cerebral cortex. Cereb Cortex. 18:2352–2357.

Van Essen DC. 1997. A tension-based theory of morphogenesis and compact wiring in the central nervous system. Nature. 385:313–318.

White T, Su S, Schmidt M, Kao C-Y, Sapiro G. 2010. The development of gyrification in childhood and adolescence. Brain Cogn. 72:36.

Zilles K, Armstrong E, Schleicher A, Kretschmann HJ. 1988. The human pattern of gyrification in the cerebral cortex. Anat Embryol (Berl). 179:173–179.

Zilles K, Palomero-Gallagher N, Amunts K. 2013. Development of cortical folding during evolution and ontogeny. Trends Neurosci. 36:275–284.